C−F Bond Activation by the 14-Electron $M(X)(PH_3)_2$ (M = Rh, Ir; X = CH_3, H, Cl) Complex. A Density Functional Study

Ming-Der Su* and San-Yan Chu*

Contribution from the Department of Chemistry, National Tsing Hua University, Hsinchu 30043, Taiwan, ROC

Received April 21, 1997. Revised Manuscript Received July 11, 1997[⊗]

Abstract: The oxidative addition of the F−CH_3 bond to coordinatively unsaturated *trans*-$M(X)(PH_3)_2$ (M = Rh, Ir; X = CH_3, H, Cl) was theoretically investigated by density functional theory. All of the stationary points were determined at the B3LYP/LANL2DZ level. A configuration mixing model based on the theory of Pross and Shaik has been used to develop an explanation for the barrier height as well as the reaction enthalpy. Our theoretical findings suggest that the singlet−triplet splitting ($\Delta E_{st} = E_{triplet} - E_{singlet}$) of the ML_3 species can be used as a basis to predict its reaction activity for oxidative additions; i.e., the smaller the ΔE_{st} of ML_3, the lower the barrier height and the larger the exothermicity, in turn, the faster the oxidative addition reaction. Considering the substituent effect, and the nature of the central metal, the following conclusions therefore emerge: for the 14-electron *trans*-$M(X)(PH_3)_2$ complex, a stronger π-donor ligand (such as Cl) as well as a heavier transition metal center (the third-row) will result in a smaller ΔE_{st}, and thus will provide a potential model for the oxidative addition of saturated C−F bonds. In this work, an energetically feasible reaction mechanism which should not have radical intermediates involved is suggested.

I. Introduction

Halogenated hydrocarbons are important industrial compounds used as solvents, as dry-cleaning agents, as refrigerants, and in the etching of microelectronic chips.[1,2] This widespread usage has led to their existence in the environment as pollutants.[3,4] A major class of substitution compounds are hydrofluorocarbons (HFCs), fluorinated short-chain alkanes. Because they contain no chlorine or bromine, HFCs were initially assumed to be ozone friendly. Subsequently, concerns were raised that HFCs could still pose a threat to the environment because their infrared-absorbing properties make them potential greenhouse gases, and their atmospheric lifetimes are critical elements for evaluating their global warming potentials.[5] This lent urgency to research on the catalytic defluorination of HFCs.[6,7]

Our goal in this work is to find potential transition metal complexes that are able to activate saturated C−F bonds. Since it has been observed[8] that Ir(I) alkylphosphine complexes are capable of oxidative addition to some of the strongest polar bonds (e.g., H−OH, 119 kcal/mol; Cl−Si, 112 kcal/mol), this has prompted us to investigate the reaction of 14-electron d^8 $M(X)(PH_3)_2$ with HFCs.[9] The other reason for choosing low-valent C−F activating complexes is because, as Crabtree has pointed out,[10] 14-electron complexes have advantages over 16-electron species from the point of view of building a catalyst system. Thus, a study of the important C−F activation reaction, eq 1, was undertaken.

$$\textit{trans}\text{-}M(X)(PH_3)_2 + F{-}CH_3 \rightarrow \textit{trans}\text{-}M(X)(PH_3)_2(F)(CH_3) \quad (1)$$

For the present, the focus is on C−F activation by 14-electron complexes of the form $M(X)(PH_3)_2$, where M = Rh and Ir and X = CH_3, H, and Cl.[11]

In this work we investigate the important features of reaction 1 by using fluoromethane (CH_3F) as a model HFC. The C−F and C−H bonds in CH_3F are roughly the same strength (108 ± 3[12] and 101 ± 1[13] kcal/mol, respectively), and it should be pointed out that our focus on the activation of the C−F bond of CH_3F does not imply that the C−H bond is not important. It means only that we admit the complexity of the problem and choose to treat the C−F activation aspects separately. Hence, in order to reduce the complexity of the problem we choose a simple system ($ML_3 + CH_3F$) in which the determining variable is the efficiency of oxidative additions. C−H bond activation can be considered later as an effect which may or may not affect the C−F insertion.

[⊗] Abstract published in *Advance ACS Abstracts,* October 1, 1997.

(1) Cobourn, J. W.; Winters, H. F. *J. Vac. Sci. Technol.* **1979**, *16*, 391.

(2) (a) Gottscho, R. A.; Smolinsky, G.; Burton, R. H. *J. Appl. Phys.* **1982**, *53*, 5908. (b) Smolinsky, G.; Gottscho, R. A.; Abys, S. A. *Ibid*. **1983**, *54*, 3582.

(3) (a) Senkan, S. M. *Chem. Eng. Prog.* **1987**, *12*, 58. (b) Senkan, S. M. *Environ. Sci. Technol*. **1988**, *22*, 368. (c) Rodriquez, C. F.; Bohme, D. K.; Hopkinson, A. C. *J. Phys. Chem.* **1996**, *100*, 2942. (d) Papasavva, S.; Illinger, K. H.; Kenny, J. E. *J. Phys. Chem.* **1996**, *100*, 10100.

(4) (a) Crutzen, P. J. *Angew. Chem., Int. Ed. Engl.* **1996**, *35*, 1758. (b) Molina, M. J. *Ibid.* **1996**, *35*, 1778. (c) Rowland, F. S. *Ibid.* **1996**, *35*, 1787.

(5) A salient measure of the contribution of HFCs in this regard is the total absolute infrared intensity in the atmospheric window to terrestrial blackbody radiation, A_{min}, in the frequency range 700−1500 cm^{-1}. See ref 4.

(6) Saunders, G. C. *Angew. Chem., Int. Ed. Engl.* **1996**, *35*, 2615.

(7) Burdeniuc, J.; Jedlicka, B.; Crabtree, R. H. *Chem. Ber*. **1997**, *130*, 145 and references therein.

(8) (a) Milstein, D.; Calabrese, J. C.; Williams, I. D. *J. Am. Chem. Soc.* **1986**, *108*, 6387. (b) Zlota, A. A.; Frolow, F.; Milstein, D. *J. Chem. Soc., Chem. Commun.* **1989**, 1826.

(9) It was concluded that the fluoride affinity of highly electrophilic early transition metals tends to preclude their use in catalysis. Similarly, the alkali and alkaline earth metals are not suitable as C−F activation catalysts due to their propensity to form ionic salts with fluoride. Consequently, Richmond et al. suggested that further developments should be sought employing low-valent electron-rich transition metals. See: Kiplinger, J. L.; Richmond, T. G.; Osterberg, C. E. *Chem. Rev.* **1994**, *94*, 373 and references therein.

(10) Crabtree, R. H. In *Activation and Functionalization of Alkanes*; Davies, J. A., Ed., VCH: New York, 1990; p 69.

(11) For a theoretical study of C−H activation of methane by 14-electron d^8 ML_3 complexes, see: (a) Koga, N.; Morokuma, K. *J. Phys. Chem.* **1990**, 94, 5454. (b) Koga, N.; Morokuma, K. *J. Am. Chem. Soc*. **1993**, *115*, 6883. (c) Cundari, T. R. *J. Am. Chem. Soc.* **1994**, *116*, 340. (d) Margl, P.; Ziegler, T.; Blochl, P. E. *J. Am. Chem. Soc.* **1995**, *117*, 12625.

(12) Botor, J. P.; Edwards, J. G. *J. Chem. Phys.* **1984**, *81*, 2185.

(13) Crepin, C.; Verges, J.; Amiot, C. *Chem. Phys. Lett*. **1984**, *122*, 10.

S0002-7863(97)01269-9 CCC: $14.00

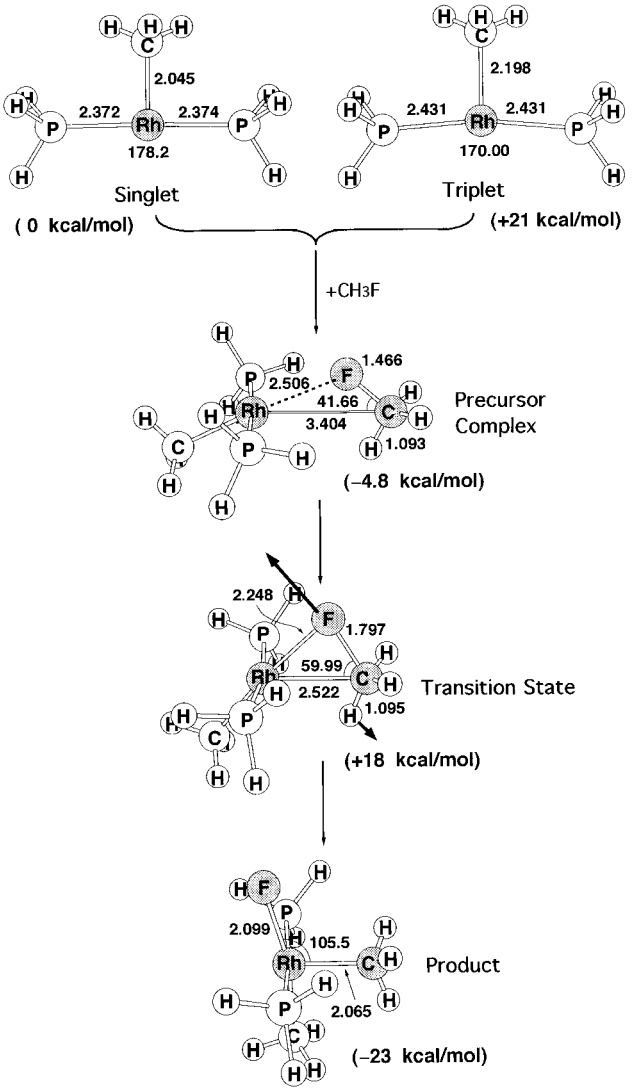

Figure 1. B3LYP/LANL2DZ optimized geometries (in angstroms and degrees) of the reactants (singlet and triplet), precursor complex, transition state, and product of *trans*-Rh(CH3)(PH3)2. Values in parentheses are the relative energies at the B3LYP/LANL2DZ level. The heavy arrows indicate the main atomic motions in the transition state eigenvector.

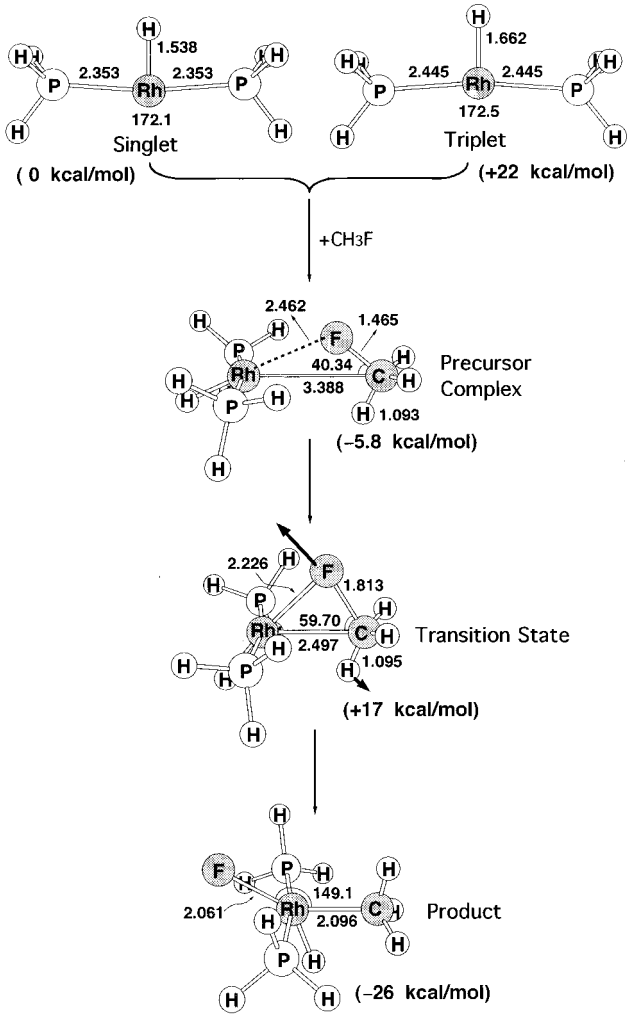

Figure 2. B3LYP/LANL2DZ optimized geometries (in angstroms and degrees) of the reactants (singlet and triplet), precursor complex, transition state, and product of *trans*-Rh(H)(PH3)2. Values in parentheses are the relative energies at the B3LYP/LANL2DZ level. The heavy arrows indicate the main atomic motions in the transition state eigenvector.

No previous theoretical study has to our knowledge been published on the activation of saturated C−F bonds by transition metal complexes. In the present paper we report potential energy profiles for oxidative addition of F−CH_3 to the 14-electron M(X)$(PH_3)_2$ species (i.e., eq 1) using density functional theory (DFT). Details of the calculations are given in the Appendix. Section II presents the results of geometry optimization for stationary points. Several crucial results deduced from the potential energy profiles are given in section III. The origin of the barrier heights and reaction enthalpies for oxidative addition of coordinatively unsaturated transition metal complexes is discussed in section IV. Section V contains brief concluding remarks.

II. Geometries and Energetics of M(X)$(PH_3)_2$ + CH_3F

In this section the results for four regions on the potential energy surfaces will be presented: 14-electron d^8 *trans*-M(X)-$(PH_3)_2$ plus free CH_3F, a precursor complex, the transition state, and the oxidative addition product *trans*-M(X)$(PH_3)_2$(F)(CH_3). The fully optimized geometries for *trans*-M(X)$(PH_3)_2$ (M = Rh, Ir; X = CH_3, H, Cl) calculated at the B3LYP/LANL2DZ level are given in Figures 1−6, respectively. Relative energies are collected in Table 1.

Several interesting results can be drawn from those figures and the table. First, let us consider the electronic structure of the coordinatively unsaturated 14-electron d^8 ML_3 reactant. An orbital energy level diagram for the ML_3 fragment is given in Scheme 1.[14] There are eight electrons to distribute among the d levels in Scheme 1. Since the splitting between the $1a_1$ and $2a_1$ levels is small, it is reasonable to deduce that the candidates for the ground state are the $^1A_1$ singlet state with electronic configuration $(a_2)^2(b_1)^2(b_2)^2(1a_1)^2(2a_1)^0$ and the $^3A_1$ triplet state with electronic configuration $(a_2)^2(b_1)^2(b_2)^2(1a_1)^1(2a_1)^1$.[11] As shown in Table 1, the B3LYP/LANL2DZ results indicate that only the M(X)$(PH_3)_2$ complex with a chlorine ligand is a triplet ground state, whereas other complexes are singlets. This is because the good π-donor, Cl, will cause the energy of b_2 to rise while keeping the energies of $1a_1$ and $2a_1$ relatively constant.[15] Namely, a better π-donor will push the energy of b_2 up closer to $2a_1$ and then the HOMO(b_2)−LUMO($2a_1$) difference will decrease. Consequently, the open-shell triplet state is of lowest energy for the *trans*-M(Cl)$(PH_3)_2$ (M = Rh

(14) Albright, T. A.; Burdett, J. K.; Whangbo, M. H. *Orbital Interaction in Chemistry*; Wiley: New York, 1985; p 339.

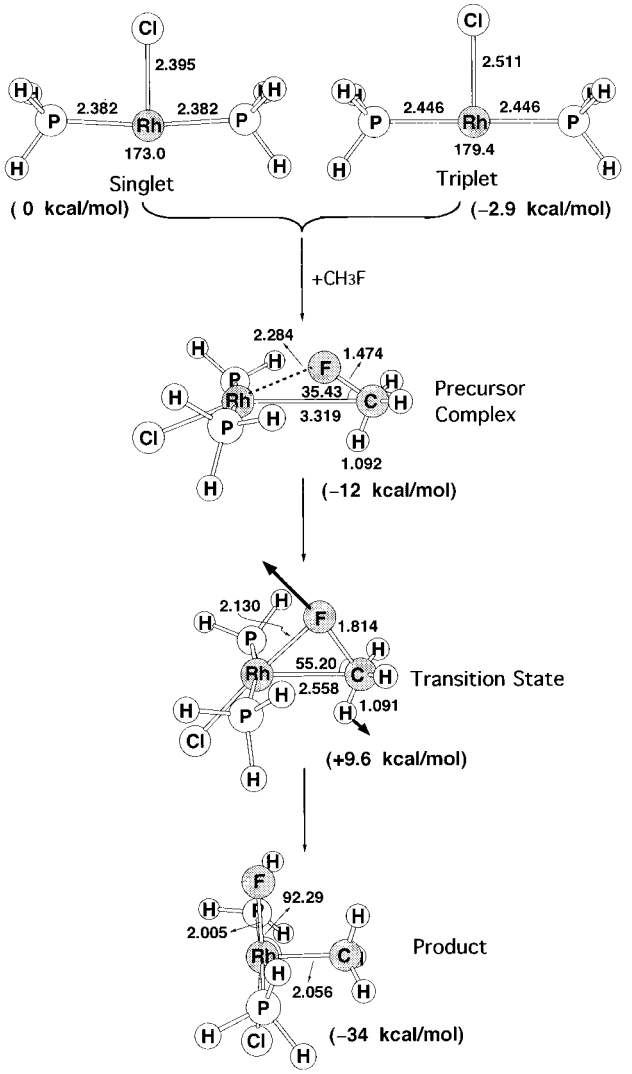

Figure 3. B3LYP/LANL2DZ optimized geometries (in angstroms and degrees) of the reactants (singlet and triplet), precursor complex, transition state, and product of *trans*-Rh(Cl)$(PH_3)_2$. Values in parentheses are the relative energies at the B3LYP/LANL2DZ level. The heavy arrows indicate the main atomic motions in the transition state eigenvector.

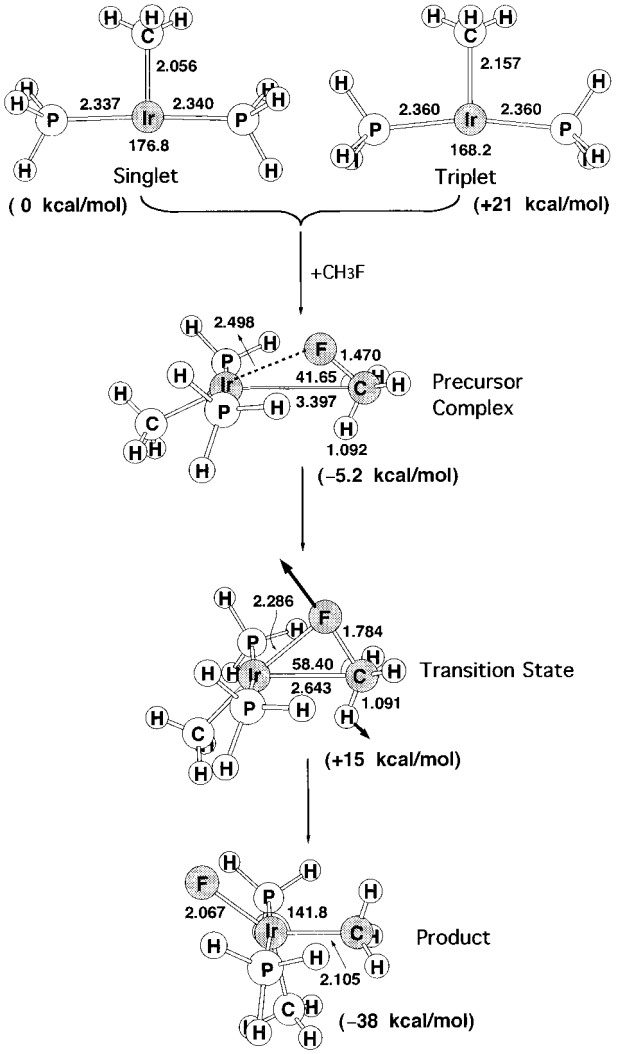

Figure 4. B3LYP/LANL2DZ optimized geometries (in angstroms and degrees) of the reactants (singlet and triplet), precursor complex, transition state, and product of *trans*-Ir$(CH_3)(PH_3)_2$. Values in parentheses are the relative energies at the B3LYP/LANL2DZ level. The heavy arrows indicate the main atomic motions in the transition state eigenvector.

and Ir) complexes. Moreover, our DFT calculations imply that Rh(Cl)$(PH_3)_2$ and Ir(Cl)$(PH_3)_2$ reactants in a triplet state might insert into the saturated C−F bond via a diradical mechanism. Nevertheless, it is well established that whenever a triplet reactant contains a heavy atom center (such as a transition metal), strong spin−orbit coupling may occur, which can provide a spin-inversion process for transferring to the singlet reactant and then undergoing the singlet reaction.[16] In addition, the results in Table 1 also suggest that the excitation energy from the triplet ground state to the first singlet state for Rh(Cl)$(PH_3)_2$ and Ir(Cl)$(PH_3)_2$ fragments is quite small; i.e., −2.9 and −4.6 kcal/mol, respectively. Both of these considerations should make the transition from the triplet to the singlet state take place without difficulty. Thus, it could well be the case that the oxidative addition reactions proceed on the singlet surface, even if the reactants start from the triplet state. We shall therefore focus on the singlet surface from now on.

Second, as in Figures 1−6, it is clear to see that, as expected for a 14-electron d^8 ML_3 complex, the geometry is T-shaped.[14] Additionally, for reactant complexes M(X)$(PH_3)_2$ (M = Rh, Ir; X = CH_3, H, Cl), the distance r(M−X) and the distance r(M−P) are found to be larger for the triplet compared to the singlet. The reason for this can be readily seen in Scheme 1. The longer M−X and M−P bonds in the triplet $^3A_1$ state reflect the fact that the antibonding interaction between the metal center and the ligands is somewhat stronger with the $2a_1$ orbital than the $1a_1$. Additionally, the S^2 expectation values of the triplet state reported in Table 1 show a negligible spin contamination, so that their geometries and energetics are reliable for the present study.

Third, as seen in Figures 1−6, all precursor complexes adopt a side-on η^2-C,F structure. In addition, the distance between carbon and the migrating fluorine in the CH_3F moiety for the precursor complexes studied here is slightly elongated (∼1.47 Å), compared to 1.45 Å in free CH_3F. The M−C distance to the CH_3F in the precursor complexes Rh$(CH_3)(PH_3)_2$·CH_3F, Rh(H)$(PH_3)_2$·CH_3F, Ir$(CH_3)(PH_3)_2$·CH_3F, and Ir(H)$(PH_3)_2$·CH_3F

(15) (a) The triplet d^8 M(Cl)$(PH_3)_2$ complex will have the configuration $(a_2)^2(b_1)^2(1a_1)^2(b_2)^1(2a_1)^1$, with the corresponding term $^3B_2$. (b) However, Ziegler et al. found that the ground state of Rh(Cl)$(PH_3)_2$ is $^1A_1$ at the DFT level (see ref 11d), while Koga and Morokuma concluded that the ground state of Rh(Cl)$(PH_3)_2$ should be $^3A_1$, which could be labeled wrong, based on MP4SDTQ results (see ref 11a).

(16) (a) Su, M.-D. *Chem. Phys. Lett*. **1995**, *237*, 317. (b) Su, M.-D. *J. Org. Chem*. **1995**, *60*, 6621. (c) Su, M.-D. *J. Phys. Chem.* **1996**, *100*, 4339. (d) Su, M.-D. *Chem. Phys*. **1996**, *205*, 277. (e) Su, M.-D. *J. Org. Chem*. **1996**, *61*, 3080.

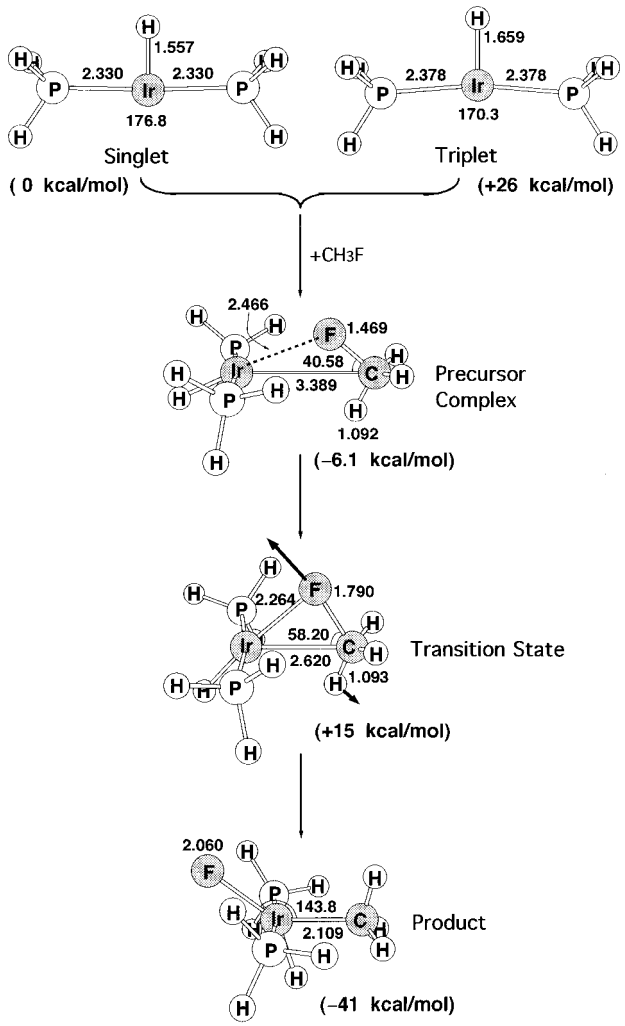

Figure 5. B3LYP/LANL2DZ optimized geometries (in angstroms and degrees) of the reactants (singlet and triplet), precursor complex, transition state, and product of *trans*-Ir(H)$(PH_3)_2$. Values in parentheses are the relative energies at the B3LYP/LANL2DZ level. The heavy arrows indicate the main atomic motions in the transition state eigenvector.

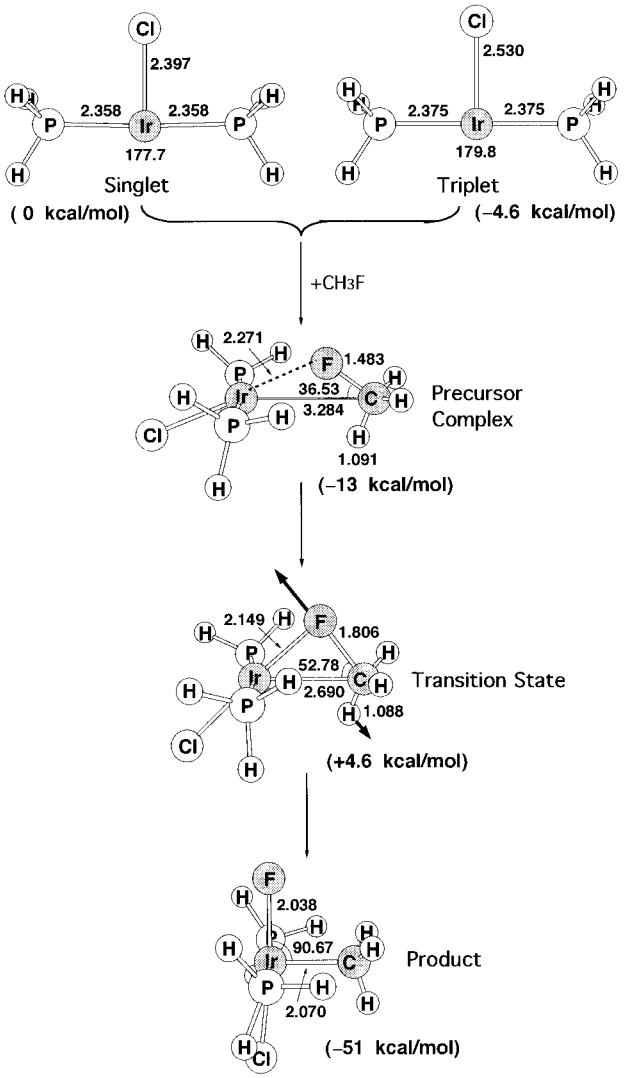

Figure 6. B3LYP/LANL2DZ optimized geometries (in angstroms and degrees) of the reactants (singlet and triplet), precursor complex, transition state, and product of *trans*-Ir(Cl)$(PH_3)_2$. Values in parentheses are the relative energies at the B3LYP/LANL2DZ level. The heavy arrows indicate the main atomic motions in the transition state eigenvector.

is 3.40, 3.39, 3.40, and 3.39 Å, respectively, whereas Rh(Cl)$(PH_3)_2$·CH_3F and Ir(Cl)$(PH_3)_2$·CH_3F have a M−C distance of 3.32 and 3.28 Å, respectively. We attribute the weak intermediate bond and long M−C distance in the first four precursor complexes to the stronger trans-destabilizing effect of CH_3 and H compared to Cl.[17] Furthermore, as shown in Table 1, in the first step the reactants yield a precursor complex with a stabilization energy of 12 and 13 kcal/mol at the B3LYP/LANL2DZ level for Rh(Cl)$(PH_3)_2$ and Ir(Cl)$(PH_3)_2$, respectively, which is twice as large as that for Rh$(CH_3)(PH_3)_2$ (4.8 kcal/mol), Rh(H)$(PH_3)_2$ (5.8 kcal/mol), Ir$(CH_3)(PH_3)_2$ (5.2 kcal/mol), and Ir(H)$(PH_3)_2$ (6.1 kcal/mol). Thus, the longer M−C distance correlates with a smaller value for the intermediate stabilization energy.

Fourth, the optimized transition state structures together with arrows indicating the main atom motion in the transition state eigenvector are shown in Figures 1−6, respectively. All six transition states show the same three-center pattern involving metal, carbon, and fluorine atoms. Such characteristic three-center transition states have been observed in oxidative additions of C−H bonds to 16-electron CpML as well as 14-electron ML_2 systems.[18] Examination of the single imaginary frequency for each transition state provides excellent confirmation of the insertion process, the C−F bond stretching with the fluorine migrating to the metal center. Moreover, the geometrical structures of the transition states reflect the fact that the lone pairs of electrons on the fluorine interact with the empty s/p/d hybridized orbital (i.e., the LUMO, $2a_1$ in Scheme 1) on the central metal. The four-electron repulsion is minimized when the M(X)$(PH_3)_2$ lone pair (i.e., the HOMO, $1a_1$ in Scheme 1) is directed away from the migrating fluorine.

Fifth, our theoretical results given in Figures 1−6 reveal that all of the products M(X)$(PH_3)_2$(F)(CH_3) adopt a trigonal bipyramidal geometry, in which two phosphine ligands occupy the axial sites of the trigonal bipyramid. We admit that such 5-coordinated products might be just local minima on the energy surface. Thus, it is possible for them to undergo fluxional rearrangement, either of the Berry pseudorotation or the turnstile type, to reach the global minimum. Such studies, however, are beyond the scope of the present work.

(17) Burdett, J. K.; Albright, T. A. *Inorg. Chem.* **1979**, *18*, 2112.

(18) (a) For 16-electron CpML systems, see: Su, M.-D.; Chu, S.-Y. *Organometallics* **1997**, *16*, 1621. (b) For 14-electron ML_2 systems, see: Su, M.-D.; Chu, S.-Y. Submitted.

Table 1. Relative Energies for Singlet and Triplet *trans*-M(X)$(PH_3)_2$ Fragments and for the Process *trans*-M(X)$(PH_3)_2$ + F−CH_3 → Precursor Complex → Transition State → Product[a]

system	singlet (kcal/mol)	ΔE_{st}[b,c] (kcal/mol)	reactant (kcal/mol)	ΔE_{int}[d] (kcal/mol)	ΔE_{act}[e] (kcal/mol)	ΔH[f] (kcal/mol)
Rh$(CH_3)(PH_3)_2$	0	+21.4 [2.006]	0	−4.78	+17.8	−22.9
Rh(H)$(PH_3)_2$	0	+21.5 [2.004]	0	−5.85	+17.4	−25.9
Rh(Cl)$(PH_3)_2$	0	−2.91 [2.006]	0	−11.5	+9.63	−33.9
Ir$(CH_3)(PH_3)_2$	0	+20.6 [2.003]	0	−5.21	+15.3	−38.3
Ir(H)$(PH_3)_2$	0	+26.2 [2.003]	0	−6.10	+14.7	−41.3
Ir(Cl)$(PH_3)_2$	0	−4.63 [2.004]	0	−13.3	+4.62	−50.8

[a] At the B3LYP/LANL2DZ level. [b] Energy relative to the corresponding singlet state. A negative value means that the triplet is the ground state. [c] The value within square brackets is the S^2 expectation value. [d] The stabilization energy of the precursor complex, relative to the corresponding reactants. [e] The activation energy of the transition state, relative to the corresponding reactants. [f] The exothermicity of the product, relative to the corresponding reactants.

Scheme 1

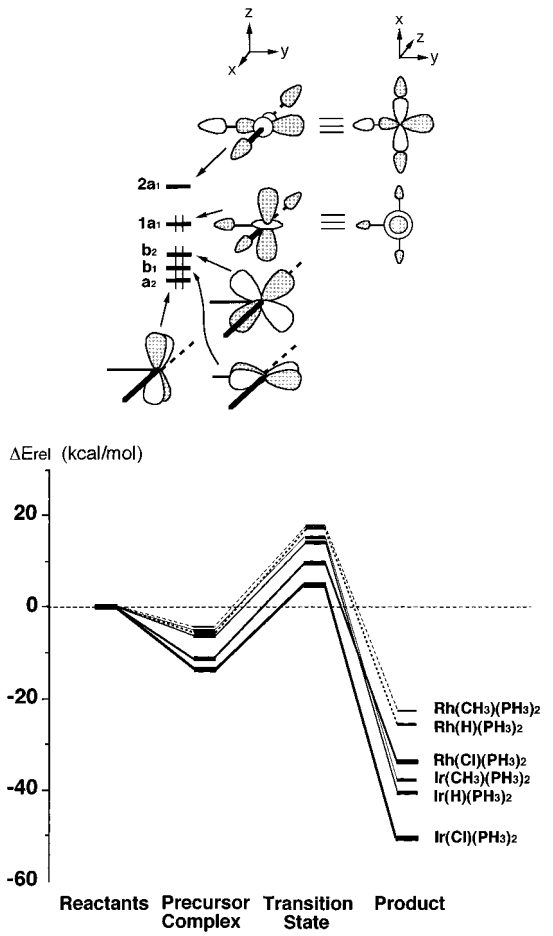

Figure 7. Potential energy surfaces for the activation of the F−CH_3 bond by *trans*-M(X)$(PH_3)_2$ (M = Rh, Ir; X = CH_3, H, Cl). The relative energies are taken from the B3LYP/LANL2DZ values as given in Table 1. For optimized structures of the stationary points, see Figures 1−6.

III. Discussion of the Potential Energy Surfaces

The potential energy profiles based on the data in Table 1 are summarized in Figure 7. Four interesting conclusions can be drawn from this figure.

First, it is clearly seen that, for the same metal center, the better π-donor the ligand X, the lower the activation energy and the larger the exothermicity for the oxidative addition of F−CH_3 to M(X)$(PH_3)_2$ complexes (left to right in Figure 7). For instance, as demonstrated in Table 1, since the Cl ligand is a stronger π-donor than CH_3 and H, the barrier height for F−CH_3 activation with M = Rh increases in the order Rh(Cl)$(PH_3)_2$ (9.6 kcal/mol) < Rh(H)$(PH_3)_2$ (17 kcal/mol) < Rh$(CH_3)(PH_3)_2$ (18 kcal/mol) and, for M = Ir, Ir(Cl)$(PH_3)_2$ (4.6 kcal/mol) < Ir(H)$(PH_3)_2$ (15 kcal/mol) ∼ Ir$(CH_3)(PH_3)_2$ (15 kcal/mol). It is noteworthy that the activation barriers for the Ir reactions are smaller than those for their Rh analogues.

Second, it is clear that all of the oxidative addition reactions are thermodynamically exothermic. The order of exothermicity follows the same trend as the activation energy: Rh(Cl)$(PH_3)_2$ (−34 kcal/mol) < Rh(H)$(PH_3)_2$ (−26 kcal/mol) < Rh$(CH_3)(PH_3)_2$ (−23 kcal/mol) and Ir(Cl)$(PH_3)_2$ (−51 kcal/mol) < Ir(H)$(PH_3)_2$ (−41 kcal/mol) < Ir$(CH_3)(PH_3)_2$ (−38 kcal/mol). Again, the Ir reactions are more exothermic than their Rh counterparts.

Third, our model calculations also suggest that oxidative additions involving a third-row transition metal (such as Ir) should be preferable to those of a second-row transition metal (such as Rh) since it is demonstrated not only that the former are thermodynamically more favorable but also that the kinetic barriers associated with them are typically small.[19] On the other hand, the reductive elimination (right to left in Figure 7) of the second-row metal is more favorable than that of the third-row homologue.

Fourth, the transition state studies based on the model systems we have used here strongly suggest that radical intermediates should not be involved in C−F activation reactions for the 14-electron d^8 ML_3 cases. Moreover, the energetics shown in Figure 7 indicate that our model reactions actually have low activation energies for activation of the C−F bond by coordinatively unsaturated M(X)$(PH_3)_2$ complexes. For example, the activation barrier relative to the corresponding reactants for F−CH_3 insertion to Ir(Cl)$(PH_3)_2$ was calculated at the B3LYP/LANL2DZ level to be 4.6 kcal/mol and the activation energies for the whole reactions are about 18 kcal/mol. We estimate that these barriers will be greatly improved with more complete calculations.[20] Additionally, the overall energy of this reaction is exothermic by 51 kcal/mol. In any event, the 14-electron

(19) To our knowledge, it was experimentally found that stable oxidative addition products with alkanes will be found predominantly in the third row; e.g., for oxidative addition of iridium and rhodium intermediates to alkane C−H bonds, the products formed in the latter case are much less stable and undergo reductive elimination at −20 °C. For details, see: Bergman, R. G. *Science* **1984**, *223*, 902.

(20) Calculated DFT barrier heights are often, if anything, too low; see: *Chemical Applications of Density Functional Theory*; Laird, A., Ross, R. B., Zeigler, T., Eds.; American Chemical Society: Washington, DC, 1996. We would like to thank referee B for bringing this reference to our attention.

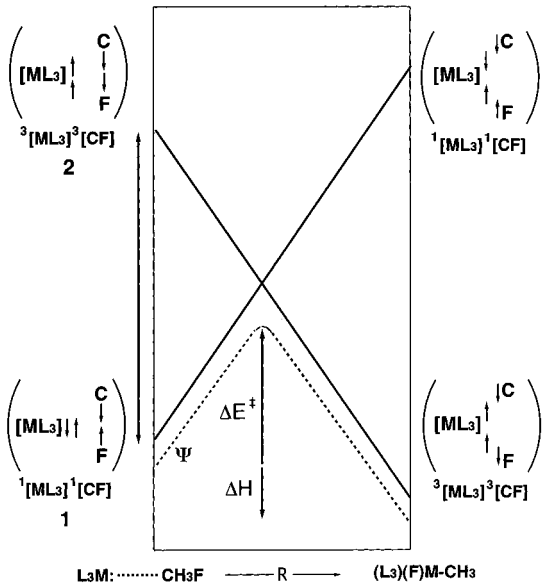

Figure 8. Energy diagram for an oxidative addition reaction showing the formation of a state curve (Ψ) by mixing two configurations: the reactant configuration (1) and the product configuration (2). It is apparent that both the activation energy ($\Delta E^{\ddagger}$) and reaction enthalpy (ΔH) are proportional to ΔE_{st} ($=E_{triplet} - E_{singlet}$ for 14-electron ML_3) and $\Delta E_{\sigma\sigma^*}$ ($=E_{triplet} - E_{singlet}$ for CH_3F). See the text.

$Ir(Cl)(PH_3)_2$ complex is a potential model for oxidative addition of saturated C−F bonds kinetically as well as thermodynamically.

As there are no relevant experimental and theoretical data on such systems, the above results are predictions.

IV. The Origin of the Barrier and Reaction Enthalpy for Oxidative Addition of $M(X)(PH_3)_2$

In order to investigate the reason why the barrier for $Ir(Cl)(PH_3)_2$ is lower than those for other model reactions, a simple valence bond (VB) model has been used to develop an explanation for the barrier heights discussed above.

Recently, it has been found[21,22] that a configuration mixing (CM) model, based on the work of Pross and Shaik,[23] can successfully explain the origin of the barrier height as well as the reaction enthalpy for oxidative addition reactions of transition metal complexes.[24] In the oxidative addition reaction, it may exist in a number of predetermined states, each of which may be approximated by the appropriate electronic configuration.[25] However, there are only two predominant configurations that contribute significantly to the total wave function Ψ and, in turn, affect the shape of the potential energy surface. (See Figure 8.) One is the reactant ground state configuration that ends up as an excited configuration in the product region. The other is the excited configuration of the reactants that correlates with the ground state of the products.

The key VB configurations for ML_3 oxidative addition are illustrated in **1** and **2**, while the key MO configurations are illustrated in **3** and **4**.[22b] The VB configuration **1**, labeled

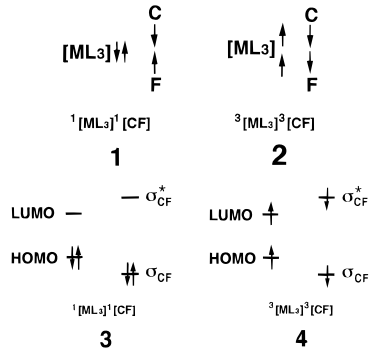

$^1[ML_3]^1[CF]$, is termed the reactant configuration because this configuration is a good descriptor of the reactants; the two electrons on the ML_3 moiety are spin-paired to form the lone pair while the two electrons on the CH_3F moiety are spin-paired to form a C−F σ bond. On the other hand, configuration **2** is the VB product configuration. Note that the spin arrangement is now different. The electron pairs are coupled to allow both M−F and M−C bond formation and simultaneous C−F bond breaking. In order to obtain this configuration from the reactant configuration **1**, each of the two origin electron pairs needs to be uncoupled. Namely, those two electron pairs require excitation from the singlet state to the triplet state. Hence, this configuration is labeled $^3[ML_3]^3[CF]$. It should be noticed that $^3[ML_3]^3[CF]$ is an overall singlet configuration, despite the fact that it contains within it two local triplets. The MO representations of VB configurations **1** and **2** are shown in **3** and **4**, respectively. It is the avoided crossing of these two configurations that leads to the simplest description of the ground state energy profiles for oxidative addition reactions of 14 electron ML_3 complexes.[21,22]

As shown in Figure 8, it is apparent that the barrier height ($\Delta E^{\ddagger}$) as well as the reaction enthalpy (ΔH) may be expressed in terms of the initial energy gap between the reactant and product configurations. In other words, the reactivity of such oxidative additions will be governed by the singlet−triplet excitation energies for each of the reactants, i.e., ΔE_{st} ($=E_{triplet} - E_{singlet}$ for 14-electron ML_3) and $\Delta E_{\sigma\sigma^*}$ ($=E_{triplet} - E_{singlet}$ for CH_3F). Accordingly, if $\Delta E_{\sigma\sigma^*}$ is a constant, then a smaller value of ΔE_{st} leads to (1) reduction of the reaction barrier since the intended crossing of $^1[ML_3]^1[CF]$ and $^3[ML_3]^3[CF]$ is lower in energy and (2) a larger exothermicity since the energy of the product is now lower than that of the reactant. In short, *the smaller the ΔE_{st} of ML_3, the lower the barrier height and the larger the exothermicity, in turn, the faster the oxidative addition reaction*.

Our model calculations confirm the above prediction. For the B3LYP/LANL2DZ calculations on the six systems studied here, a plot of activation barrier versus ΔE_{st} is given in Figure 9: the best fit is $\Delta E^{\ddagger} = 0.339\Delta E_{st} + 8.59$. Likewise, the linear correlation between ΔE_{st} and the reaction enthalpy (ΔH), also obtained at the same level of theory, is $\Delta H = 0.356\Delta E_{st} - 40.4$. This investigation provides strong evidence that the singlet−triplet splitting can be used as a guide to predict the reactivity of the reactants. Thus, in order to find a good model for the facile oxidative addition of C−F bonds, an understanding of the singlet−triplet splitting ΔE_{st} of the coordinatively unsaturated 14-electron ML_3 is crucial.

(21) Su, M.-D. *Inorg. Chem.* **1995**, *34*, 3829.

(22) (a) Su, M.-D.; Chu, S.-Y. *J. Am. Chem. Soc.* **1997**, *119*, 5373. (b) Su, M.-D.; Chu, S.-Y. *J. Phys. Chem.* in press.

(23) (a) Shaik, S.; Schlegel, H. B.; Wolfe, S. *Theoretical Aspects of Physical Organic Chemistry*; John Wiley & Sons Inc.: New York, 1992. (b) Pross, A. *Theoretical and Physical Principles of Organic Reactivity*; John Wiley & Sons Inc.: New York, 1995.

(24) It has been shown (ref 21) that the CM model can be used to understand the origin of barrier heights for carbene insertion reactions. Since 14-electron ML_3 is known to be isolobal to CH_2:, it is in principle conceivable that, using the "isolobal analogy" (see: Hoffmann, R. *Angew. Chem., Int. Ed. Engl.* **1982**, *21*, 711), the same predictions could also be applied to organometallic systems.

(25) For instance, there could exist the first excited triplet state $^3[ML_3]^1[CF]$ and the second excited triplet state $^1[ML_3]^3[CF]$. Since we are only concerned with singlet states and both $^3[ML_3]^1[CF]$ and $^1[ML_3]^3[CF]$ are triplet states, it can be assumed that $^3[ML_3]^1[CF]$ and $^1[ML_3]^3[CF]$ contribute very little, if at all, to the total wavefunction Ψ. See ref 21.

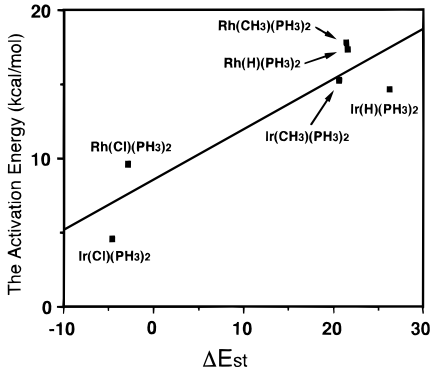

Figure 9. ΔE_{st} ($=E_{triplet} - E_{singlet}$) for *trans*-M(X)$(PH_3)_2$ (M = Rh, Ir; X = CH_3, H, Cl) fragments (see the third column in Table 1) vs the activation energy for oxidative addition of *trans*-M(X)$(PH_3)_2$ fragments to F−CH_3 (see the sixth column in Table 1). The linear regression equation is $\Delta E^{\ddagger} = 0.339\ \Delta E_{st} + 8.59$, with a correlation coefficient $R = 0.82$. All values were calculated at the B3LYP/LANL2DZ level. See the text.

Considering the substituent effect qualitatively, since oxidative addition involves charge transfer from the metal center of M(X)$(PH_3)_2$ to the incoming F−CH_3, an electron-donating X which can increase the electron density on the central metal would stabilize the transition state and lower the barrier height. We can conclude that both CH_3 and H ligands are better electron donors than some electron-withdrawing ligands (such as CO, NO) and are therefore more favorable for oxidative additions. Nevertheless, when X in *trans*-M(X)$(PH_3)_2$ is replaced by chlorine, which is a relatively stronger π-donor, though a weaker σ-donor, its HOMO−LUMO energy gap is reduced, and this favors the high-spin state.[14] Consequently, the 14-electron *trans*-M(Cl)$(PH_3)_2$ complex is expected to have a triplet ground state, leading to a smaller singlet−triplet splitting ΔE_{st} ($=E_{triplet} - E_{singlet}$), which has been confirmed by our calculations as shown earlier. It is therefore anticipated that *a 14-electron trans-M(X)L_2 complex with a better π-donor ligand X would lead to a smaller ΔE_{st} and, in turn, allow a more facile oxidative addition to the saturated C−F bond.*

Considering the nature of the central metal, our model calculations have shown that oxidative addition to Ir(X)$(PH_3)_2$ has a lower activation energy than that to Rh(X)$(PH_3)_2$. The reason for this can also be traced back to the singlet−triplet splitting of M(X)$(PH_3)_2$. As Siegbahn has pointed out,[26] the Ir atom has a quartet d^7s^2 ground state with a high excitation energy to the doublet d^9 state of 61 kcal/mol. For the Rh atom, the ground state is quartet d^8s^1 but with a relatively low excitation energy to the doublet d^9 state of 7.8 kcal/mol. This implies that Ir would prefer to remain in a high-spin state, whereas Rh favors a low-spin state. As such, it is reasonabe to conclude that the promotion energy from the singlet state to the triplet state, used to form the strongest covalent bonds, should be smaller for the Ir complex than for the Rh complex. For this reason, *insertion into a C−F bond is a more facile and exothermic process for the Ir system than for its Rh counterpart*.

V. Conclusion

Our work has shown that the singlet−triplet splitting ΔE_{st} ($=E_{triplet} - E_{singlet}$) based on a configuration mixing model can provide a useful basis for understanding and rationalizing the relative magnitude of the activation barriers as well as reaction enthalpies for oxidative addition of C−F bonds to 14-electron d^8 *trans*-M(X)$(PH_3)_2$. With the above analysis in mind, we are confident in predicting that *for 14-electron d^8 trans-M(X)$(PH_3)_2$ systems, a stronger π-donating ligand X (such as Cl) and a heavier transition metal (i.e., third-row) will lead to a smaller ΔE_{st} and, in turn, will facilitate oxidative addition reactions to saturated C−F bonds*. Moreover, from our study we believe that a concerted process, which does not involve radical intermediates, should play an important role in C−F bond activation reactions by transition metal complexes. In spite of simplicity, our approach can provide chemists with important insights into the factors controlling the activation of saturated C−F bonds and thus permit them to predict the reactivity of several, as yet unknown, 14-electron d^8 *trans*-M(X)$(PH_3)_2$ intermediates.

We are eagerly awaiting experimental results.

Acknowledgment. We are thankful to the National Center for High-Performance Computing of Taiwan and the Computing Center at Tsing Hua University for generous amounts of computing time. We also thank the National Science Council of Taiwan for financial support. We wish to thank Professor H. B. Schlegel for providing useful software. We are grateful to the referees (especially referee B) for critical comments and helpful corrections of the manuscript.

Note Added in Proof. As suggested by referees, to support the B3LYP/LANL2DZ barriers studied in this work, several single-point calculations were performed by adding polarization functions in the basis set. Recently, Morokuma and coworkers[33] reported that the B3LYP/II//B3LYP/I approach is nearly as good as CCSD(T)/II//B3LYP/II. Basis set I stands for LANL2DZ, while basis set II is obtained by adding to basis set I polarization p-, d-, and f-functions for hydrogen,[34] the main group elements,[35] and the transition metals,[36] respectively. We thus recalculated the energies shown in Table 1 at the B3LYP/LANL2DZ optimized geometries using the basis set II described above. Their relative B3LYP/II//B3LYP/I energies are collected in Table 2. Compared to the B3LYP/I results shown in Table 1, those energies are, in principle, qualitatively consistent with each other. For instance, a linear relationship between ΔE_{st} and the activation energy $\Delta E^{\ddagger}$, as well as the reaction enthalpy ΔH, can also be obtained. For the Rh case, $\Delta E^{\ddagger} = 0.374\Delta E_{st} + 16.0$ and $\Delta H = 0.469\Delta E_{st} - 23.3$; for the Ir case, $\Delta E^{\ddagger} = 0.265\Delta E_{st} + 11.6$ and $\Delta H = 0.265\Delta E_{st} - 40.0$. Indeed, the

(26) Siegbahn, P. E. M. *J. Am. Chem. Soc.* **1996**, *118*, 1487.

(27) (a) Becke, A. D. *Phys. Rev. A* **1988**, *38*, 3098. (b) Lee, C.; Yang, W.; Parr, R. G. *Phys. Rev. B* **1988**, *37*, 785. (c) Becke, A. D. *J. Chem. Phys*. **1993**, *98*, 5648.

(28) Ricca, A.; Bauschlicher, C. W. *Theor. Chim. Acta*. **1995**, *92*, 123.

(29) Hay, J. P.; Wadt, W. R. *J. Chem. Phys.* **1985**, *82*, 299.

(30) Hay, J. P.; Wadt, W. R. *J. Chem. Phys.* **1985**, *82*, 284.

(31) Gaussian 94, Revision B.2: M. J. Frisch, G. W. Trucks, H. B. Schlegel, P. M. W. Gill, B. G. Johnson, M. A. Robb, J. R. Cheeseman, T. Keith, G. A. Peterson, J. A. Montgomery, K. Raghavachari, M. A. Al-Laham, V. G. Zakrzewski, J. V. Ortiz, J. B. Foresman, J. Cioslowski, B. B. Stefanov, A. Nanayakara, M. Challacombe, C. Y. Peng, P. Y. Ayala, W. Chen, M. W. Wong, J. L. Andres, E. S. Replogle, R. Gomperts, R. L. Martin, D. J. Fox, J. S. Binkley, D. J. Defrees, J. Baker, J. P. Stewart, M. Head-Gordon, C. Gonzalez, and J. A. Pople, Gaussian, Inc., Pittsburgh PA, 1995.

(32) Dunning, T. H.; Hay, P. J. *Modern Theoretical Chemistry*; Schaefer, H. F., Ed.; Plenum: New York, 1976; pp 1−28.

(33) (a) Musaev, D. G.; Morokuma, K. *J. Phys. Chem*. **1996**, *100*, 6509. (b) Cui, Q.; Musaev, D. G.; Morokuma, K. *Organometallics*, **1997**, *16*, 1355.

(34) (a) Dunning, T. H., Jr. *J. Chem. Phys*. **1970**, *53*, 2823. (b) Dunning, T. H., Jr.; Hay, P. J. *Methods of Electronic Structure Theory*; Schaefer, H. F., III, Ed.; Plenum Press: New York, 1977; Vol. 2.

(35) (a) For C and F, see ref 34. (b) For P and Cl, see: Magnusson, E.; Schaefer, H. F., III *J. Chem. Phys.* **1985**, *83*, 5721.

(36) Ehlers, A. W.; Bohme, M.; Dapprich, S.; Gobbi, A.; Hollwarth, A.; Jonas, V.; Kohler, K. F.; Stegmann, R.; Veldkamp, A.; Frenking, G. *Chem. Phys. Lett*., **1993**, *208*, 111.

Table 2. Relative Energies for Singlet and Triplet *trans*-M(X)(PH$_3$)$_2$ Fragments and for the Process *trans*-M(X)(PH$_3$)$_2$ + F−CH$_3$ → Precursor Complex → Transition State → Product[a]

system	singlet (hartrees)	ΔE_{st}[b] (kcal/mol)	reactant (hartrees)	ΔE_{int}[c] (kcal/mol)	ΔE_{act}[d] (kcal/mol)	ΔH[e] (kcal/mol)
Rh(CH$_3$)(PH$_3$)$_2$	0	+24.3	0	−3.64	+25.4	−8.03
Rh(H)(PH$_3$)$_2$	0	+25.9	0	−4.70	+25.3	−14.8
Rh(Cl)(PH$_3$)$_2$	0	+2.65	0	−9.03	+16.9	−22.3
Ir(CH$_3$)(PH$_3$)$_2$	0	+49.0	0	−4.10	+22.7	−28.0
Ir(H)(PH$_3$)$_2$	0	+29.4	0	−4.17	+22.8	−30.4
Ir(Cl)(PH$_3$)$_2$	0	+5.07	0	−11.0	+11.5	−39.4

[a] At the B3LYP/II//B3LYP/I level, see the text. [b] Energy relative to the corresponding singlet state. A negative value means that the triplet is the ground state. [c] The stabilization energy of the precursor complex, relative to the corresponding reactants. [d] The activation energy of the transition state, relative to the corresponding reactants. [e] The exothermicity of the product, relative to the corresponding reactants.

addition of polarization functions will certainly change the internuclear distances and may affect the calculated energy gaps, especially the singlet−triplet energy differences. However, since our GAUSSIAN94/DFT package so far is unable to handle the derivatives of f orbitals, the optimized geometries cannot thus be obtained at the B3LYP/II level. It is therefore difficult for us to assess the validity of the B3LYP/II//B3LYP/I calculations in this work, and the relative energies shown in Table 2 can only be considered as references. Nevertheless, with the above analysis, we believe that polarization functions do not affect results in a meaningful fashion and that double-ζ basis sets are adequate for the present study.

Appendix

All geometries were fully optimized without imposing any symmetry constraints, although in some instances the resulting structure showed various elements of symmetry. For our DFT calculations, we used the hybrid gradient-corrected exchange functional proposed by Becke,[27a,b] combined with the gradient-corrected correlation functional of Lee, Yang, and Parr.[27c] This functional is commonly known as B3LYP and has been shown to be quite reliable both for geometries and energies.[28]

Effective core potentials (ECPs) were used to represent the 28 innermost electrons of rhodium (up to the 3d shell).[29] Likewise, ECPs were used to represent the 60 innermost electrons of the iridium (up to the 4f shell) atom.[29] For phosphorus and chlorine we also used the Hay and Wadt relativistic ECP.[30] For these atoms, the basis set was that associated with the pseudopotential, with a standard LANL2DZ contraction.[31] For hydrogen, carbon, and oxygen atoms the double ζ-basis of Dunning−Huzinaga was used.[32] We denote our B3LYP calculations by B3LYP/LANL2DZ.

Vibrational frequencies at stationary points were calculated at the B3LYP/LANL2DZ level of theory to identify them as minima (zero imaginary frequencies) or transition states (one imaginary frequency). All calculations were performed with the GAUSSIAN94/DFT package.[31]

JA971269U